

## Original article

# Suitability evaluation of CO<sub>2</sub> sequestration in saline aquifers: Insights from regional basin studies

Shiguo Wu<sup>1,2,3</sup>\*, Yuan Chen<sup>4</sup>\*, Xueqing Zhou<sup>2</sup>, Qiang Chen<sup>5</sup>, Linqi Zhu<sup>6</sup>, Lizhong Wang<sup>3</sup>

<sup>1</sup>College of Marine Science and Technology, Hainan Tropical Ocean University, Sanya 572022, P. R. China

<sup>2</sup>Institute of Deep-sea Science and Engineering, Chinese Academy of Sciences, Sanya 572000, P. R. China

<sup>3</sup>Hainan Research Institute of Zhejiang University, Sanya 572025, P. R. China

<sup>4</sup>Sinopec Petroleum Exploration and Production Research Institute, Beijing 100083, P. R. China

<sup>5</sup>China Southern Petroleum Exploration & Development Corporation, PetroChina, Haikou 570100, P. R. China

<sup>6</sup>Department of Earth Science and Engineering, Imperial College London, London SW7 2BP, United Kingdom

### Keywords:

CO<sub>2</sub> sequestration  
saline aquifers  
sequestration site selection  
mechanical responses

### Cited as:

Wu, S., Chen, Y., Zhou, X., Chen, Q., Zhu, L., Wang, L. Suitability evaluation of CO<sub>2</sub> sequestration in saline aquifers: Insights from regional basin studies. *Advances in Geo-Energy Research*, 2026, 20(1): 43-55.  
<https://doi.org/10.46690/ager.2026.04.04>

### Abstract:

The growing severity of global climate change has highlighted the importance of CO<sub>2</sub> sequestration as a key strategy for reducing CO<sub>2</sub> emissions and mitigating global warming. To this end, sedimentary basins worldwide contain extensive yet underexplored saline aquifers with substantial sequestration potential for long-term CO<sub>2</sub> sequestration. In this study, the suitability and mechanical responses of CO<sub>2</sub> sequestration in a representative half-graben saline aquifer were systematically unraveled through integrated theoretical analysis and multi-physics-coupled numerical simulations. Key factors, such as temperature, pressure, reservoir properties, and caprock distribution, were evaluated based on well logging and mud logging data. Taking the evaluation results as a basis, optimal reservoir-caprock combinations were identified and classified into three types according to their spatial distribution: Single caprock-reservoir, lower interlayer-caprock-reservoir, and upper interlayer-caprock-reservoir. To simulate the mechanical responses during CO<sub>2</sub> injection and sequestration, corresponding conceptual models were developed. The results indicate that Type III reservoir-caprock combinations, featuring upper mudstone interlayers, exhibit the lowest caprock stress, reduced leakage risk and enhanced sequestration security, which should be prioritized in sequestration site selection. Our findings provide valuable insights for selecting safe and effective CO<sub>2</sub> sequestration sites in saline aquifers across regional sedimentary basins.

## 1. Introduction

Carbon capture, utilization and storage is a promising strategy to mitigate global climate change. Therein, CO<sub>2</sub> captured from industrial sources is transported to designated geological formations for long-term sequestration. Among the various geological options, saline aquifers are the most promising candidates due to their widespread distribution and substantial storage potential (Gorecki et al., 2009). While these

formations offer pathways for long-term CO<sub>2</sub> sequestration through structural, residual, dissolved, and mineral trapping, ensuring the safety and efficiency of sequestration requires rigorous site selection and characterization. Given the complexity of subsurface CO<sub>2</sub> behavior, sequestration sites must meet stringent criteria regarding geological characteristics, environmental impact, economic viability, as well as social acceptance (Kumar et al., 2020).

Offshore sedimentary basins, often characterized by ex-

**Table 1.** Safety evaluation indicator system for CO<sub>2</sub> sequestration sites (Gorecki et al., 2009).

Indicators	Favorable conditions	Unfavorable conditions	Importance
Reservoir-caprock combination	Medium to good with multiple sets	Poor and discontinuous	Decisive
Pressure condition	Pressure gradient < 12 MPa	Pressure gradient > 14 MPa	Decisive
Monitoring condition	Existing	Lacking	Decisive
Water source impact	No	Yes	Decisive
Seismic activity	Medium to weak	Strong	Necessary
Fracture density	Medium to sparse	Dense	Necessary
Hydrological condition	Medium to regional flow system	Short flow system connected to water source	Necessary
Depth	> 800 m	< 750 ~ 800 m	Ideal
Geothermal condition	< 35 °C/m	≥ 35 °C	Ideal
Temperature	≥ 35 °C	< 35 °C	Ideal
Pressure	≥ 7.5 MPa	< 7.5 MPa	Ideal
Thickness of reservoir	≥ 20 m	< 20 m	Ideal
Porosity	≥ 10%	< 10%	Ideal
Permeability	≥ 20 mD	< 20 mD	Ideal
Thickness of caprock	≥ 10 m	< 10 m	Ideal
Well density	Medium to low	High	Ideal

tensive hydrocarbon exploration and well-developed infrastructure, offer favorable conditions for CO<sub>2</sub> sequestration. However, prior studies in these basins have mainly focused on oil and gas exploitation, while systematic assessments of CO<sub>2</sub> sequestration suitability – a critical component of carbon capture, utilization, and storage deployment – remain limited (Li et al., 2015; Qin et al., 2023; Zhou et al., 2024). To address this gap, various evaluation frameworks have been developed, typically involving a set of key indicators, including storage capacity, injectivity, sealing capability, and operability (Rutqvist, 2012; Chen et al., 2025). For offshore sites, additional considerations include seawater temperature and pressure (Tomić et al., 2018). Holloway (1997) highlighted the cost-saving advantages of repurposing depleted oil and gas fields due to their existing infrastructure and proven capacity. Van der Meer (1992) first proposed an approach to estimate sequestration capacity using a series of suitability indicators such as reservoir porosity and permeability, and caprock thickness, and established a prediction model based on fluid dynamics. Bachu (2003) proposed a systematic evaluation system for the assessment of CO<sub>2</sub> sequestration potential at regional and basin scales. This system incorporates 15 key indicators such as basin scale, structural characteristics, buried depth, hydrogeological and lithological conditions, and geothermal gradients, providing a comprehensive basis for evaluating sequestration suitability. This work established a structured methodology for integrating geological, hydrodynamic and thermal factors into site screening, laying the foundation for subsequent CO<sub>2</sub> storage assessment systems and has been widely regarded as a milestone in the development of screening methodologies. Gibson-Poole et al. (2008) adapted

Bachu's system to Australian geological conditions by incorporating reservoir-caprock combination indicators and excluding emission-sources-related parameters, thereby emphasizing storage capacity in site selection. Chadwick et al. (2008) further refined the evaluation methodology via application to the SACS and CO2STORE projects (two CO<sub>2</sub> storage projects in Sleipner with the aim of developing research into the potential for large-scale storage of CO<sub>2</sub> in underground saline aquifer formations). Subsequently, the International Energy Agency Greenhouse Gas Research and Development Programme (IEAGHG) standardized these screening criteria and proposed recommended threshold ranges for key indicators (Gorecki et al., 2009), enhancing consistency in site suitability assessment practices, as shown in Table 1. This system classifies indicators into three categories: (1) Decisive indicators, which are critical to site feasibility; failure to meet any of these leads to immediate exclusion; (2) necessary indicators that allow some flexibility; a site may be excluded if two or more of these are unmet, while a single unmet indicator warrants further investigation; (3) ideal indicators that enhance overall suitability; the more of these that are satisfied and the more their values exceed recommended thresholds, the more suitable the site is for CO<sub>2</sub> sequestration. Raza et al. (2016) put forward a screening framework addressing key parameters including suitable storage site selections, which covers most important parameters, including injectivity, trapping mechanisms, and strength of containments. Li et al. (2015) designed a scoring table for ranking the suitability of oil fields for CO<sub>2</sub> storage to investigate the geological conditions of on- and offshore sedimentary basins in Korea and evaluated the suitability of the basins for geological CO<sub>2</sub> storage. Overall,

the evolution from Bachu's work (Bachu, 2003) to IEAGHG reflects a transition from conceptual framework development to operational standardization and international harmonization.

While these criteria are vital for initial basin-scale screening, they primarily rely on static geological and petrophysical parameters, therefore may not fully capture the dynamic risks associated with the injection process, particularly the geomechanical response of the subsurface. CO<sub>2</sub> injection inevitably elevates pore pressure, altering the *in-situ* stress state and inducing deformation in both the reservoir and the caprock (Rutqvist, 2012). This can lead to surface uplift and, critically, may compromise caprock integrity or cause fault reactivation, increasing the risk of CO<sub>2</sub> leakage (Nordbotten et al., 2005; Chen et al., 2023). Environmental assessments have also highlighted that pressure buildup can fracture reservoirs and drive CO<sub>2</sub> into overlying groundwater systems. Birkholzer and Zhou (2009) investigated the basin-scale hydrogeologic impacts of industrial-scale CO<sub>2</sub> injection using a regional three-dimensional model of the Illinois Basin, demonstrating that large-scale pressure buildup and brine migration may limit effective storage capacity and pose potential risks to caprock integrity.

Studies involving numerical simulations and field monitoring have extensively confirmed the significant mechanical responses at sequestration sites. For instance, at the In Salah site in Algeria, the world's largest onshore CO<sub>2</sub> storage site, the surface uplifted by approximately 18.6 mm three years after CO<sub>2</sub> injection (Rutqvist et al., 2010), and further simulation results indicated that the ground above the injection point uplifted by about 1.2 cm (Rutqvist, 2012). Hao et al. (2015) used the CO<sub>2</sub> Geological Storage-Coupled Thermal, Hydro, Chemical, and Mechanical (THCM) program to simulate the mechanical response after CO<sub>2</sub> injection at the In Salah site in Algeria and explored the influence of different injection methods on surface displacement. Similarly, in the Venice area, fluid injection into sandstone aquifers at a depth of 600-800 m caused a 30 cm uplift (Abbott, 2004; Castelletto et al., 2008). Rahman et al. (2022) conducted a numerical simulation analysis of surface deformation after CO<sub>2</sub> injection at the Horda platform in the Smeaheia area of the Norwegian North Sea. The results showed that surface deformation at the site could reach 7 cm after 50 years of injection and storage. To manage these risks, advanced monitoring techniques, such as Interferometric Synthetic Aperture Radar, have been employed to detect millimeter-level surface deformation (Rutqvist et al., 2002; Vasco et al., 2008). Notably, CO<sub>2</sub> injection projects were eventually suspended due to concerns regarding caprock integrity and fracture propagation. These cases underscore the critical importance of incorporating geomechanical risk assessment into site selection and long-term storage evaluation. These studies further highlight that the magnitude and pattern of deformation are highly dependent on site-specific geological structures; the magnitude of the uplift is not only linked to the injection volume and injection rate but also closely related to the injection point location, reservoir structure and geological characteristics (Mathieson et al., 2009; Onuma and Ohkawa, 2009).

Despite that studies have extensively targeted suitability

screening criteria and geomechanical risks for sequestration, these two aspects are often treated as largely independent steps in existing workflows. Suitability evaluations commonly rely on static geological parameters, while geomechanical safety is usually assessed separately using numerical simulations, with limited interaction between the two. This separation is particularly problematic for high-temperature and high-pressure reservoirs, where coupled multi-physical effects can significantly influence both sequestration feasibility and long-term stability.

To address this gap, this study presents an integrated evaluation workflow that explicitly links static suitability screening with dynamic geomechanical analysis. Static geological indicators are first used to constrain reservoir and define key input parameters, which are then incorporated into geomechanical simulations to evaluate long-term stability and safety. This methodology is applied to the Fushan Depression in the South China Sea, a representative half-graben saline aquifer characterized by high-temperature and high-pressure conditions. By systematically analyzing the geological, petrophysical and thermodynamic parameters, the optimal reservoir-caprock combinations can be classified. Furthermore, conceptual models are developed to simulate the spatiotemporal evolution of stress and uplift during CO<sub>2</sub> injection. The findings provide a theoretical basis and practical guidelines for selecting safe and effective CO<sub>2</sub> sequestration sites in the Fushan Depression and similar complex sedimentary basins.

## 2. Regional geological settings

The Beibuwan Basin is located in the northern South China Sea margin, encompassing parts of the Northern Bay Area, southern Leizhou Peninsula, and northern Hainan Island. It covers a total area of approximately 35,000 km<sup>2</sup>, with around 16,000 km<sup>2</sup> on land (Wei et al., 2024). Tectonically, it lies within the Eurasian Plate and is classified as a rifting basin in the South China. It comprises three primary structural units, arranged from north to south as: The northern depression, the western uplift, and the southern depression. Within these, there are seven secondary depressions and three in-basin uplifts, as shown in Fig. 1.

Located at the southeastern margin of the Beibuwan Basin, the Fushan Depression is a typical half-grabens structure within the Mesozoic-Cenozoic rift system of the South China Sea. It is a NE-E trending depression covering approximately 2,920 km<sup>2</sup>. The Cenozoic sedimentary sequence exceeds 9,000 m in thickness and includes, from bottom to top, the Cretaceous, the Paleogene Changliu Formation, the Liushagang Formation, the Weizhou Formation, Neogene, and Quaternary sediments. Among these, the Weizhou Formation comprises rapidly deposited fluvial sediments, characterized by light gray, interbedded sand and mud layers with a thickness of approximately 2,000 m (Wang et al., 2025). It is divided into three intervals: Ewz1, Ewz2 and Ewz3, corresponding to the sequence stratigraphic units SQwz1, SQwz2 and SQwz3, respectively (as shown in Fig. 2).

The Fushan Depression is subdivided into eight regions: BJ, BL, HC, YU, HG, YA, CY, and MT. Several oil production

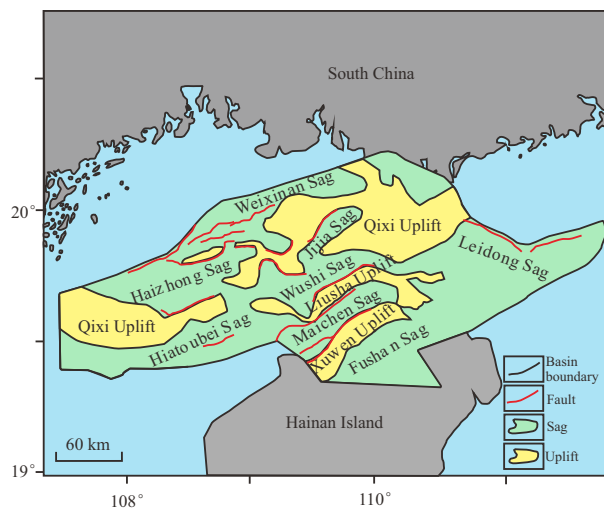


**Fig. 1.** Schematic map showing the location and tectonic division of the Beibuwan Basin between South China and Hainan Island.

wells have been drilled in this area, with main reservoirs located in the Liushagang Formation, as shown in Fig. 3. Overlying this, the Weizhou Formation mainly comprises saline aquifers, where interbedded sandstones and mudstones provide favorable caprock-reservoir combinations for potential CO<sub>2</sub> sequestration. The formation water salinity in the Fushan Depression varies considerably, generally ranging from 1,000 to 100,000 ppm, with most values concentrated between 5,000 and 25,000 ppm, indicating a moderate salinity level. Vertically, the salinity distribution is complex, while horizontally, it varies slightly across different strata. The Weizhou Formation typically exhibits higher and more uniform salinity. Existing production wells in the area could be repurposed as CO<sub>2</sub> injection wells, potentially reducing sequestration costs.

### 3. Storage suitability evaluation of CO<sub>2</sub> sequestration sites

On the basis of the IEAGHG evaluation system, the Fushan Depression was analyzed as a potential CO<sub>2</sub> sequestration site. Given its status as an active oilfield with numerous production wells, it meets both decisive and necessary indicators. This study focuses on evaluating the ideal indicators, which are categorized into three types: (1) Temperature and pressure conditions, (2) reservoir-related indicators, and (3) caprock-related indicators.

#### 3.1 Analysis of formation temperature and pressure conditions

Located in the tropical zone, the Fushan Depression is influenced by a relatively high geothermal gradient, resulting in elevated formation temperatures that are favorable for CO<sub>2</sub> sequestration. Under adequate formation pressure, high temperature facilitates the maintenance of CO<sub>2</sub> in a supercritical state, which is advantageous due to its higher density and lower viscosity. This study statistically analyzed formation temperature data from 34 wells within the Weizhou Formation (as shown in Fig. 3). The results indicate that formation

temperatures range from 38.51 °C to 125.41 °C (Fig. 4(a)), all exceeding the critical temperature of CO<sub>2</sub> (Fig. 4(b)). This confirms the presence of favorable thermal conditions for supercritical CO<sub>2</sub> sequestration. Although direct temperature data are unavailable for the CY and YU region, the buried depth of the Weizhou Formation exceeds 1,000 m. Based on regional geothermal gradients, supercritical conditions for CO<sub>2</sub> are likely achieved in these areas as well. Overall, the Weizhou Formation across the Fushan Depression meets the thermal requirements for maintaining CO<sub>2</sub> in a supercritical state.

Pressure data from 30 wells across the Fushan Depression were analyzed, revealing that the formation pressures in most reservoirs exceed the critical pressure of CO<sub>2</sub> (Fig. 5(a)). This indicates that CO<sub>2</sub> can remain in a supercritical state, facilitating its migration and long-term sequestration. However, formation pressure varies across different blocks. Although the overall buried depth of the Weizhou Formation generally satisfies the requirements for supercritical CO<sub>2</sub> sequestration, certain shallow formations, such as those in well JF2, LIAN109 and so on, exhibit pressures below the critical threshold and are therefore unsuitable as target sequestration sites. In the CY block, formation pressure shows significant variability, and intervals that meet the pressure requirements are discontinuous and scattered (Fig. 5(b)), indicating relatively low sequestration suitability. Thus, this block is not recommended for sequestration.

Considering both temperature and pressure conditions, the Weizhou Formation in the Fushan Depression generally meets the criteria for maintaining CO<sub>2</sub> in a supercritical state and is broadly suitable as a sequestration reservoir. Nevertheless, a comprehensive evaluation incorporating additional factors, such as permeability, porosity and caprock-reservoir combination, is essential to identify optimal sequestration intervals within the formation.

#### 3.2 CO<sub>2</sub> sequestration aquifers analysis

According to the CO<sub>2</sub> sequestration site evaluation criteria proposed by the IEAGHG, formations with porosity greater than 10% and permeability greater than 20 mD are considered suitable reservoir candidates. Based on well log data, porosity and permeability analyses reveal that multiple sedimentary intervals within the Weizhou Formation in the Fushan Depression meet the screening criteria, indicating the promising potential of this formation for sequestration. Reservoir thickness is a key parameter for evaluating suitability, with intervals exceeding 20 m generally regarded as ideal for CO<sub>2</sub> sequestration. The percentage of reservoirs with a thickness greater than 20 m of Ewz1, Ewz2 and Ewz3 intervals at different well locations is illustrated in Fig. 6. In most well locations (like BAO1 and JF2), the reservoir thickness meets the threshold, particularly within the Ewz1 intervals. In addition, some wells (such as JF11 and JF7) exhibit reservoirs exceeding 20 m thickness within the Ewz2 intervals (green in Fig. 6). Thick sandstones are also present in the Ewz3 intervals (pink in Fig. 6), such as LIAN36 and LIAN41.

However, not all wells have suitable sequestration formations. For example, wells HC117 and YU3 lack intervals meet-

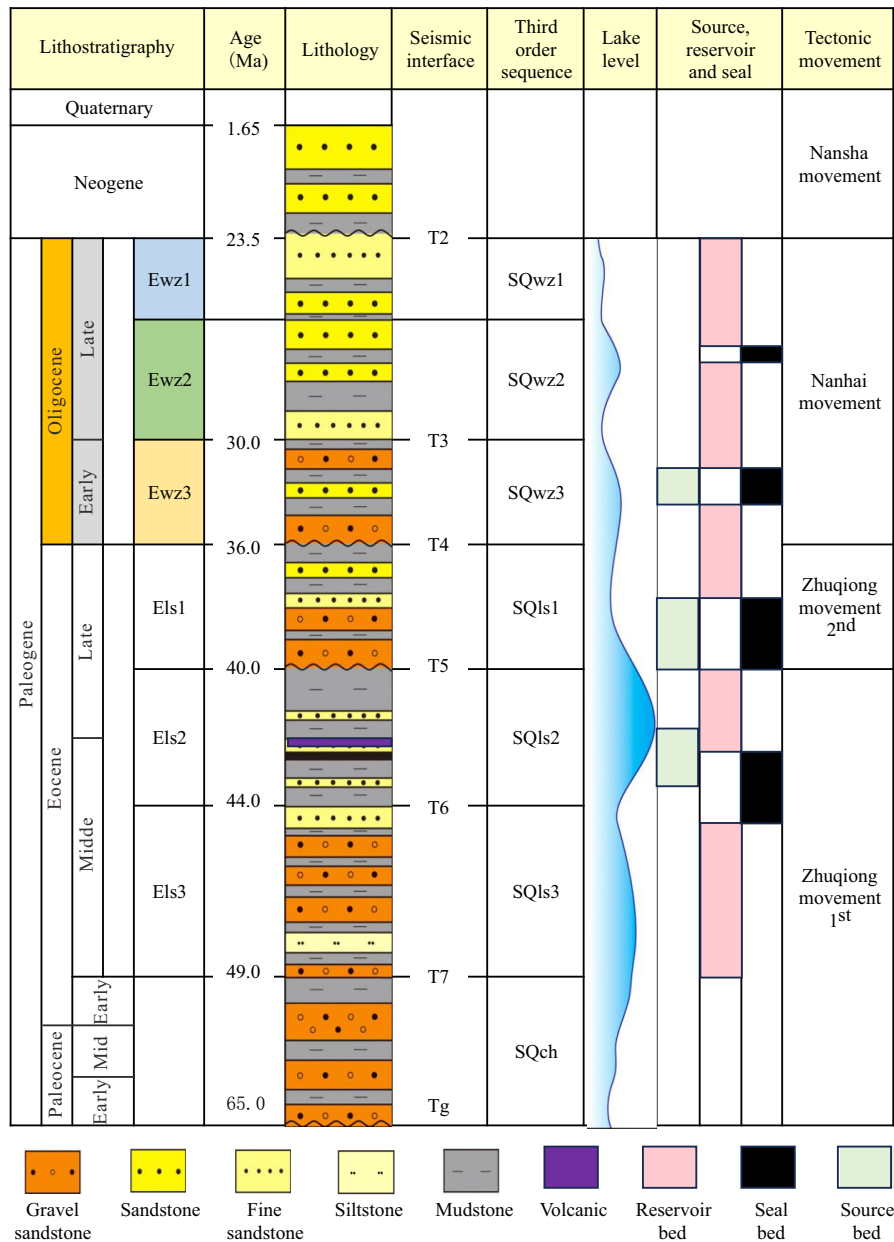


**Fig. 2.** Stratigraphic column and sequence division of the Fushan Depression in the Beibuwan Basin (revised from Liu et al. (2014), Wang et al. (2022) and Zeng et al. (2022)).

ing the required porosity, permeability or thickness thresholds. Therefore, CO<sub>2</sub> sequestration suitability must be assessed through a comprehensive evaluation of reservoir properties and their spatial distribution across the study area.

Overall, in the northeastern blocks (like BJ and BL), suitable reservoirs are predominantly located in the upper Ewz1 and Ewz2 intervals. In contrast, in the southwestern blocks (MT, CY, and HG), favorable reservoirs are mainly prevalent in the lower Ewz3. These regions generally exhibit adequate porosity, permeability and thickness, indicating strong sequestration potential. The wide spatial distribution and vertical stratification of suitable reservoirs within the Weizhou Formation provide diverse and flexible options for CO<sub>2</sub> sequestration, offering a solid foundation for site selec-

tion and future implementation.

### 3.3 Mudstone caprock analysis

In addition to favorable reservoirs, the sealing integrity critically depends on the physical properties of the overlying mudstone caprock, particularly its thickness, continuity and permeability. A low-permeability, laterally continuous caprock can effectively seal injected CO<sub>2</sub>, preventing upward migration into overlying formations or the surface, thus ensuring long-term sequestration security and minimizing environmental and geological risks. Therefore, caprock characterization, especially thickness evaluation, is a core component of site suitability assessments. However, it is intended for preliminary regional screening and cannot replace laboratory-derived br-

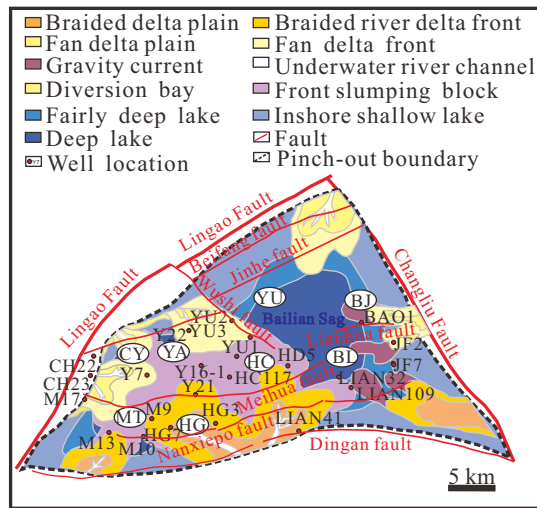


**Fig. 3.** Distribution of the depositional system, structural unit and well location of the Fushan Depression (modified after Zeng et al. (2023)).

eachthrough pressure measurements required for site-specific safety assessment.

On the basis of lithological and well log data from 28 wells in the Fushan Depression, a spatial interpolation of mudstone thickness across different intervals of the Weizhou Formation was conducted (as shown in Fig. 7) to illustrate regional trends in mudstone thickness from discrete well data, rather than to predict precise values at unsampled locations. The results show that mudstone layers are generally well developed, with total thickness ranging from 80 to 1,500 m, though significant variation exists among different layers. In the Ewz1 interval, mudstone thickness is relatively thin and spatially variable, while some discontinuities may pose a risk of local leakage; however, certain zones still exhibit moderate sealing potential. By contrast, the Ewz2 and Ewz3 intervals feature thicker and more continuous mudstone caprocks, providing more reliable sealing capacity and thus presenting preferred targets for CO<sub>2</sub> sequestration.

Block-scale analysis reveals that the BL, BJ, YU, and MT blocks exhibit generally thick and laterally continuous mudstone layers, making them favorable for CO<sub>2</sub> sequestration. In contrast, the southwestern region (particularly the HG block) shows reduced mudstone thickness and poor continuity in some wells, indicating their limited sealing potential. To ensure sequestration security in such areas, further site-specific evaluation and potentially additional engineering measurements (e.g., artificial sealing or structural reinforcement) are necessary.

To identify the optimal sequestration intervals, it is essential to analyze the vertical distribution characteristics of mudstone caprocks. On the basis of lithological and well log data, the mudstone thickness at each well was classified into three intervals: 0-5, 5-10, and > 10 m. The frequency and spatial distribution of these intervals in the three layers of the Weizhou Formation (Ewz1, Ewz2, and Ewz3) were assessed. From the perspective of sealing capacity, mudstone layers of different thicknesses serve distinct roles. Layers < 5 m thick

are generally insufficient to prevent CO<sub>2</sub> leakage, particularly under high-pressure injection, as they are prone to mechanical failure. Layers of 5-10 m exhibit moderate sealing capacity and may serve as secondary caprocks, particularly in low-volume or short-term sequestration contexts. However, they are typically inadequate as primary caprocks in large-scale sequestration projects. Mudstone layers  $\geq 10$  m, especially those  $\geq 20$  m, possess strong sealing capacity, making them suitable as primary caprocks to ensure long-term sequestration security. The distribution of mudstone thickness across different layers is illustrated in Fig. 8.

**Ewz1 layer:** This layer is generally characterized by thin mudstone layers, predominantly within the 0-5 m range, indicating poor sealing potential. However, in some well locations (such as JF2 and JF11), there are mudstone caprocks with thicknesses greater than 10 m, which can effectively seal CO<sub>2</sub>. Some well locations also have a small amount of 5-10 m mudstone layers, which can be potential secondary caprocks.

**Ewz2 layer:** This layer exhibits the most favorable sealing characteristics. In most blocks (excluding HG and CY), mudstone thickness exceeds 10 m, with several wells (such as BAO1 and LIAN32) exceeding 20 m. This suggests excellent regional sealing continuity and effectiveness, making Ewz2 the most reliable caprock interval in the Weizhou Formation.

**Ewz3 layer:** The thickness of mudstone layers is relatively small, indicating intermediate sealing capacity between Ewz1 and Ewz2. In the BJ block, mudstone thicknesses rarely exceed 10 m, indicating limited sealing reliability. However, the YU block has relatively developed mudstone layers.

Overall, mudstone thickness and continuity vary significantly across different intervals and blocks of the Weizhou Formation. Due to its thickness and continuity, the Ewz2 interval is the most suitable sequestration site, especially in the BL and HC blocks. In contrast, Ewz1 and Ewz3 generally exhibit thinner, more discontinuous mudstone layers with only a few wells, like JF2 and YU3, showing sufficient caprock conditions.

Furthermore, a comprehensive assessment of the sequestration suitability of the Weizhou Formation should consider not only mudstone thickness and continuity but also their spatial correspondence with favorable reservoirs and the prevailing temperature-pressure conditions. Thus, the tailored selection of caprock intervals across blocks and intervals is crucial to ensure long-term CO<sub>2</sub> sequestration and minimize leakage risk.

## 4. Results

Through a comprehensive analysis of the degree of adaptation of each parameter to the suitability evaluation indicator, the reservoir-caprock combinations of 28 well locations in 8 regions of Fushan Depression were determined, as shown in Fig. 9. The yellow, green and blue blocks represent Ewz1, Ewz2 and Ewz3 intervals, respectively. Blocks in black denote mudstone caprocks, while blocks in pink and red are reservoirs, all of which meet the requirements of suitability evaluation indicators. The mudstone caprocks and reservoirs formed caprock-reservoir combinations, which can be divided

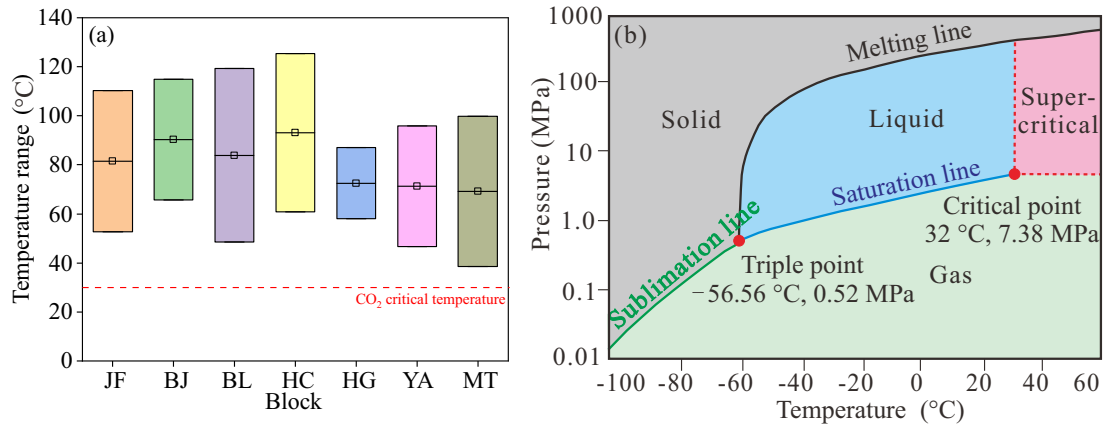


**Fig. 4.** (a) Temperature distribution across different blocks in the Fushan Depression and (b) CO<sub>2</sub> phase diagram (revised from Rochelle et al. (2009)).

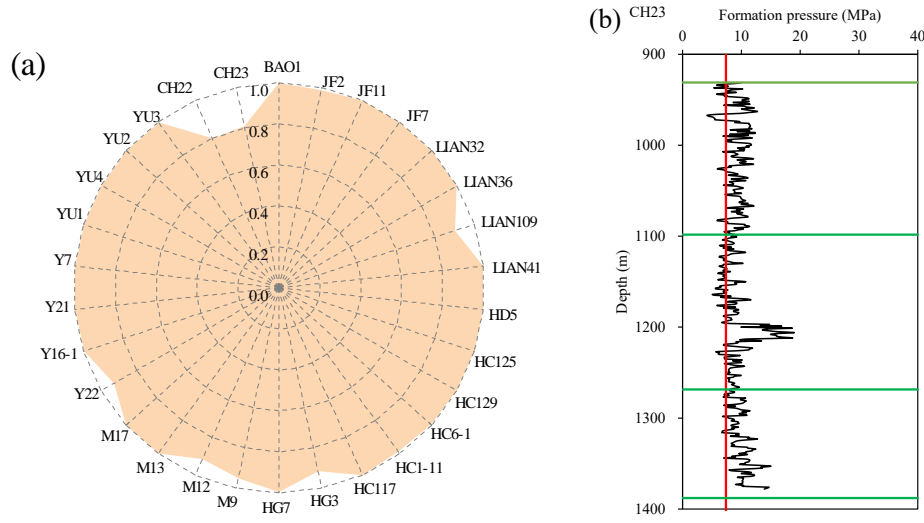


**Fig. 5.** Formation pressure analysis in the Fushan Depression wells: (a) The percentage exceeding the critical pressure of CO<sub>2</sub>, and (b) the formation pressure of Well CH23.

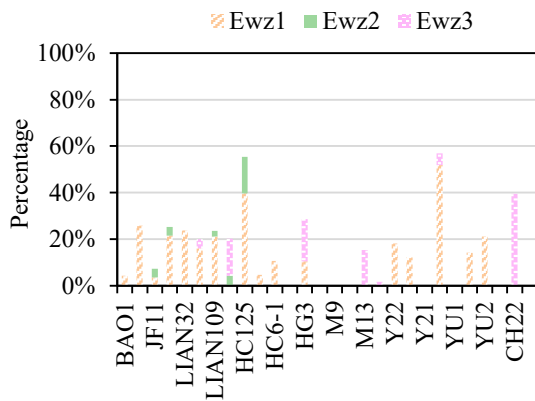


**Fig. 6.** Reservoirs with a thickness greater than 20 m in different well locations.

primary distinction between the two is the thickness of the reservoir and the caprock.

The single caprock-reservoir combination comprises a reservoir with thickness > 20 m and an overlying caprock > 10 m thick (represented by red reservoirs and black caprocks in Fig. 9). This type is characterized by favorable continuity and substantial thickness in both reservoirs and caprocks, providing strong sealing capacity. In contrast, the discontinuous multi-caprock-reservoir combination consists of multiple reservoirs with each being < 20 m thick, separated by thin mudstone interlayers (less than 5 m) and overlain by a mudstone caprock that is > 10 m thick (represented by pink reservoirs and black caprocks in Fig. 9). Based on the spatial distribution of the mudstone interlayers, this combination can be further divided into an upper interlayer-caprock-reservoir combination and a lower interlayer-caprock-reservoir combination. Although individual reservoirs are thin and discontinuous, their cumulative thickness exceeds 20 m.

into two types: (1) Single caprock-reservoir combinations and (2) discontinuous multi-caprock-reservoir combinations. The

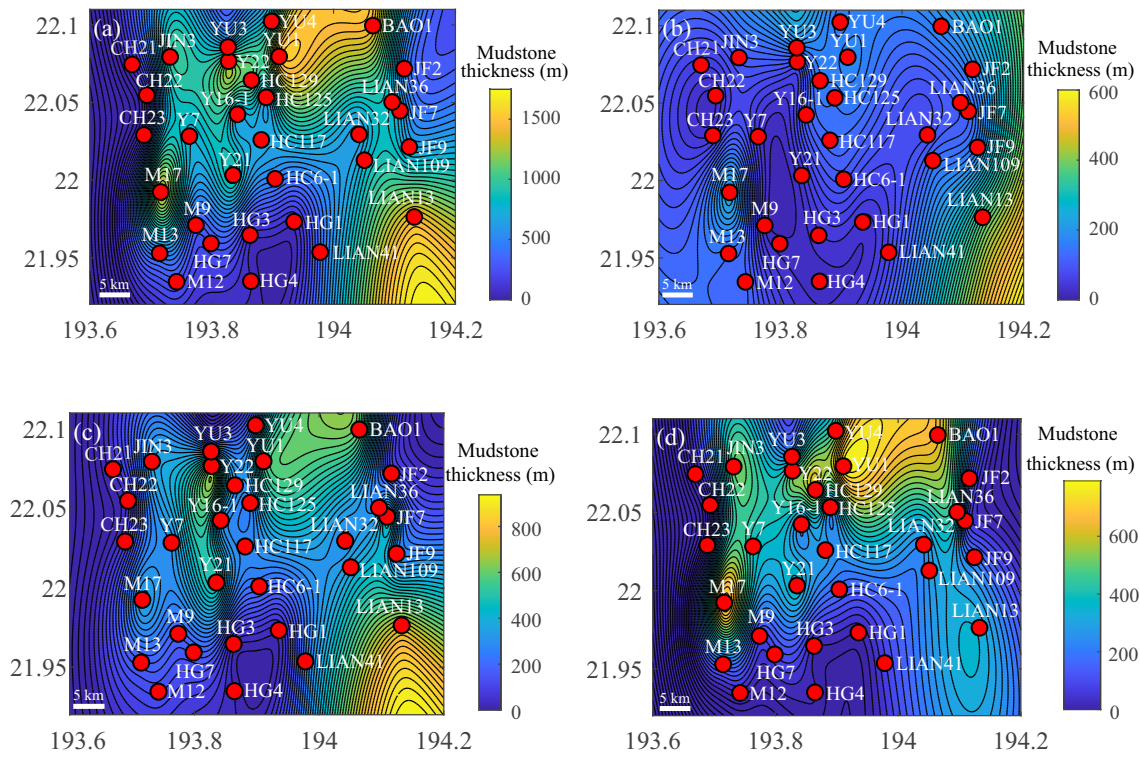


**Fig. 7.** Spatial distribution map of total mudstone thickness in different strata of the Weizhou Formation in the Fushan Depression: (a) The whole Weizhou Formation, (b) Ewz1 layer, (c) Ewz2 layer, and (d) Ewz3 layer.

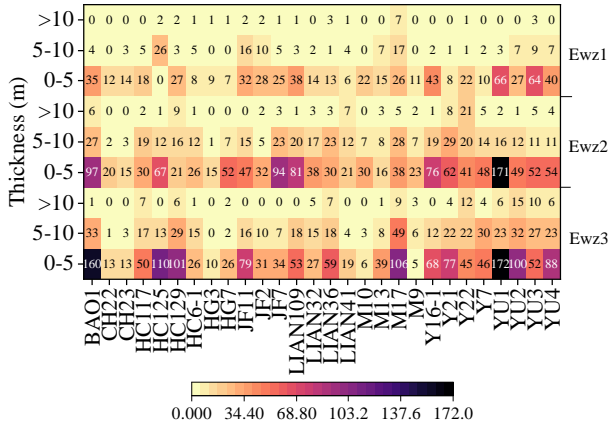


**Fig. 8.** Heatmap of the distribution of mudstone thickness categories in the Weizhou Formation at different well locations.

The mudstone interlayers help enhance the overall sealing capacity, while the presence of multiple reservoirs can compensate for the limited sequestration capacity. The performance differences between the two combinations in CO<sub>2</sub> sequestration are as follows:

(1) Sequestration capacity

The sequestration potential of the single caprock-reservoir combination is constrained by the capacity of an individual reservoir. Once the pore volume limit is reached, injection must cease. In contrast, the multi-reservoir-caprock combination benefits from cumulative sequestration capacity across multiple layers, potentially accommodating a larger volume of

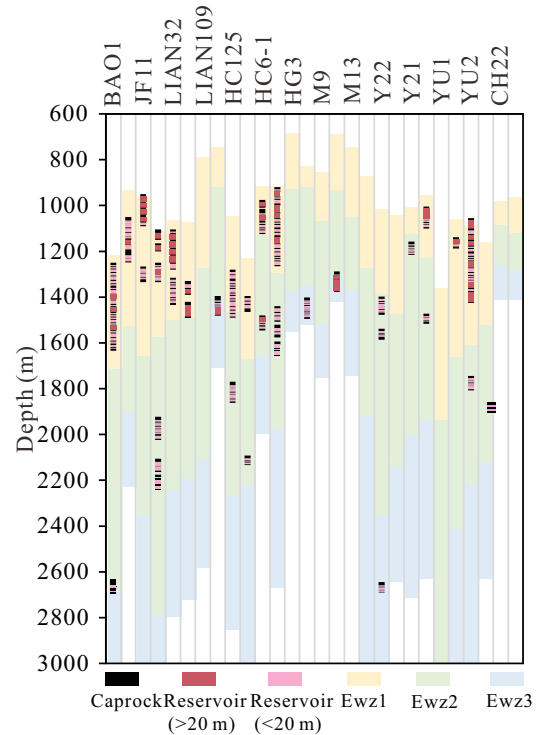


**Fig. 9.** Distribution of the reservoir-caprock combination for CO<sub>2</sub> sequestration at different well locations.

CO<sub>2</sub>.

(2) Sequestration security

The security of single combination relies on the integrity of

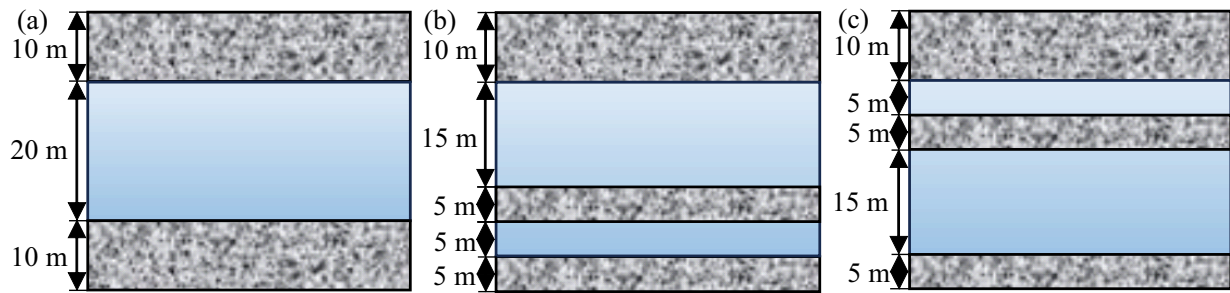


**Fig. 10.** Schematic diagram of three types of caprock-reservoir combinations for CO<sub>2</sub> sequestration in the Fushan Depression: (a) Single caprock-reservoir, (b) lower interlayer-caprock-reservoir, and (c) upper interlayer-caprock-reservoir.

one caprock, rendering it more susceptible to pressure buildup. Meanwhile, the multiple reservoir-caprock combination, with mudstone interlayer acting as secondary seals, can enhance long-term sequestration security and reduce leakage risk.

### (3) CO<sub>2</sub> migration

In a single combination, CO<sub>2</sub> migration is relatively straightforward, without complex interlayer interactions. However, pressure accumulation may influence sequestration performance. In contrast, the multiple combination may allow pressure transfer and fluid migration between layers, potentially improving CO<sub>2</sub> distribution and reducing risk of overpressure.

### (4) Monitoring and management

Monitoring a single combination is simple, focusing mainly on pressure and sequestration security within a single unit. Meanwhile, multi-combinations require a more sophisticated monitoring system to track pressure and sequestration effectiveness across each reservoir, ensuring overall stability.

Several reservoir-caprock combinations of different well locations are distributed across the Fushan Depression, mainly in the middle and upper parts of the Weizhou Formation, at depth ranging from 1,000 to 1,600 m, as shown in Fig. 9. The Ewz1 interval is dominated by single reservoir-caprock combinations, although some well locations also exhibit discontinuous multi-combinations, indicating their strong sequestration potential. In the Ewz2 interval, despite thick mudstone layers and reservoirs, many sites lack direct contact between target reservoirs and caprocks, leading to no effective reservoir-caprock combination. Only a few wells (such as those in HC and YA blocks), mostly located in the central Fushan Depression, contain discontinuous combinations. The reservoir-caprock combinations in Ewz3 are rare, with only a few discontinuous multi-combinations at well LIAN 41, HG7, M12, and Y22.

It should be noted that the identification of favorable areas in this study was based on an integrated evaluation of available geological and mechanical indicators, rather than on detailed regional planar distribution maps of individual reservoir properties such as porosity and permeability. The construction of reliable spatial distribution maps requires regionally continuous and consistently interpreted datasets, which are not currently available for all key parameters in the study area.

As a result, the present analysis emphasizes a framework-level assessment aimed at screening and comparison. Future studies could incorporate high-resolution regional distribution maps of reservoir properties to further refine the delineation of favorable areas and enhance the spatial interpretability of the assessment results.

## 5. Discussion

To evaluate the impact of reservoir-caprock configuration on CO<sub>2</sub> sequestration performance and mechanical response, three reservoir-caprock combination models were developed by the CMG-GEM (Computer Modelling Group-Generalized Equation-of-state Model) simulator based on the geological characteristics of the Fushan Depression (Fig. 10). Although the reservoir-caprock architecture in the study area is characterized by complex interbedded lithologies, the numerical models in this study adopt three simplified reservoir-caprock configurations to represent typical stratigraphic end-members distinguished by the relative position of the mudstone interlayer. This simplification is intended to capture the mechanical effects associated with different interlayer positions, rather than to reproduce fine-scale geological heterogeneity. These models incorporate four primary sequestration mechanisms: Structural, residual, dissolved, and mineral trapping.

Type I represents a single caprock-reservoir combination, simplified from the deep formation at well LIAN36. Type II is a lower interlayer-caprock-reservoir combination, based on the geological condition of well YU3, with a low-permeability mudstone interlayer being present at the lower part of the reservoir. Type III is an upper interlayer-caprock-reservoir combination, simplified from well Y7, where a low-permeability mudstone interlayer is present at the upper part of the reservoir.

In all three models, the reservoir is composed of high-strength sandstone, while the caprock and interlayer are low-strength mudstone, with the mechanical properties listed in Table 2. The top depth of each model is set at 2,700 m, with a uniform reservoir thickness of 20 m, which represents a characteristic burial depth of the target reservoir interval in the study area and corresponds to typical high-temperature and high-pressure conditions. This depth setting ensures that the applied *in-situ* stress state, temperature conditions and mechanical parameters are broadly consistent with the regional

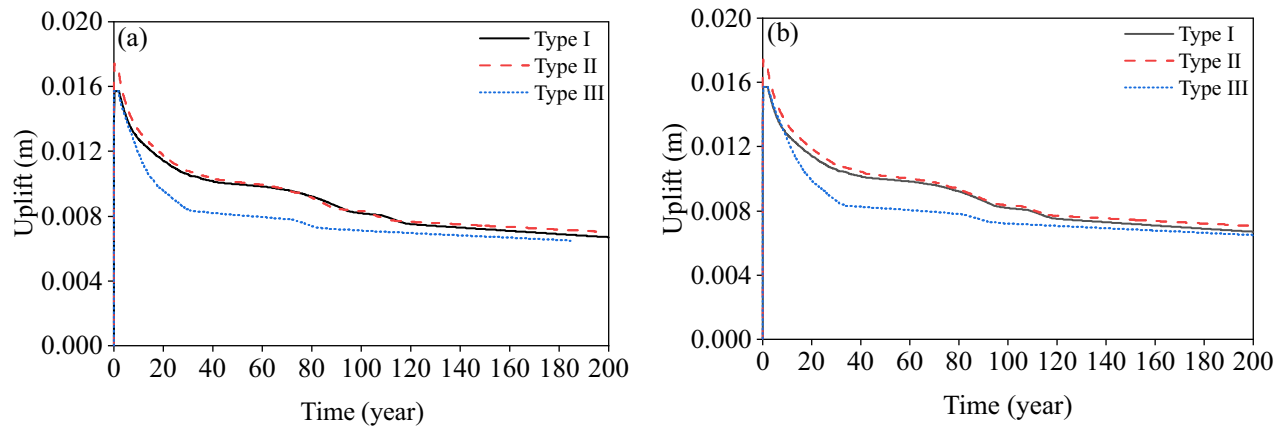


**Fig. 11.** Temporal variation of deformation in three of reservoir-caprock combinations: (a) Caprock top uplift and (b) saline aquifer top uplift.

**Table 2.** Parameters of the coupled mechanical model.

Parameters		Value
Sandstone reservoir	Young's modulus (kPa)	$1.35 \times 10^7$
	Poisson ratio (-)	0.123
	Cohesion (kPa)	2,060
Mudstone caprock and interlayer	Young's modulus (kPa)	$8.75 \times 10^6$
	Poisson ratio (-)	0.26
	Cohesion (kPa)	1,200

geological conditions, allowing for a mechanism-oriented evaluation of stress redistribution and deformation behavior under injection scenarios. The saline aquifer temperature is 96 °C; CO<sub>2</sub> is injected at a depth of 2,720-2,725 m at a rate of 500 m<sup>3</sup>/day, at a temperature of 80 °C and bottom-hole pressure of 35,000 kPa, for a duration of 2 years. The injection rate is based on typical operational scales of similar high pressure-high temperature sequestration projects in the region, balancing practical feasibility and computational efficiency. Consistent with previous studies on large-scale CO<sub>2</sub> sequestration projects, the simulation period is 200 years to evaluate long-term geomechanical and sequestration stability.

To assess the sequestration security of different reservoir-caprock combinations, a comprehensive analysis was conducted on the mechanical responses of three types of combinations during the CO<sub>2</sub> sequestration process. Fig. 11 presents the evolution of strata deformation over a 200-year period, where (a) displays the uplift at the top of the caprock and (b) shows the uplift at the top of the reservoir. It is evident that the caprock experiences slightly greater uplift than the reservoir, primarily due to the lower mechanical strength and shallower buried depth of the caprock.

According to the temporal evolution of uplift, the sequestration process can be divided into main stages:

1) Injection stage (0-2 years): Rapid CO<sub>2</sub> injection increases pore pressure inducing rock matrix expansion. Uplift oc-

curs in both the caprock and the reservoir, peaking within a short time. The maximum uplift reaches approximately 0.0173 m (caprock) and 0.0169 m (reservoir).

- 2) Early post-injection stage (2-35 years): CO<sub>2</sub> diffusion and dissolution in the formation water alleviate pressure buildup. As a result, uplift decreases progressively, though the rate of decline is much slower than the prior increase during injection.
- 3) Intermediate sequestration stage (35-120 year): Continued CO<sub>2</sub> dissolution reduces the volume of free-phase CO<sub>2</sub>, further decreasing uplift in both the reservoir and the caprock. However, the decline rate is slower than in Stage 2 and the deformation trend gradually stabilizes.
- 4) Late sequestration stage (120-200 year): Uplift remains nearly stable, with only minor reductions, and mineral trapping begins to take effect. Although mineral precipitation may alter pore structures, its influence on large-scale deformation remains limited.

Throughout the injection and sequestration process, the peak uplift (1.7 cm) is consistent in magnitude with field measurements from the In Salah CO<sub>2</sub> project (1.86 cm), supporting the reliability of the coupled multi-physics model for simulating CO<sub>2</sub>-induced deformation in saline aquifers.

The structural configuration of the reservoir-caprock combination significantly influences both the mechanical response and the sequestration security. The difference in mechanical responses among the three configurations can be mechanically attributed to the relative position of the mudstone interlayer and its role in stress redistribution and deformation partitioning within the reservoir system.

Type I: In this configuration, stress perturbations induced by injection are more uniformly transmitted through the reservoir, resulting in a relatively continuous deformation pattern.

Type II: The lower mudstone interlayer partially impedes downward stress transfer and deformation, leading to localized stress concentration above the interlayer. Consequently, uplift is slightly greater than in Type I due to enhanced stress transmission.

Type III: The upper mudstone interlayer acts as a mechan-

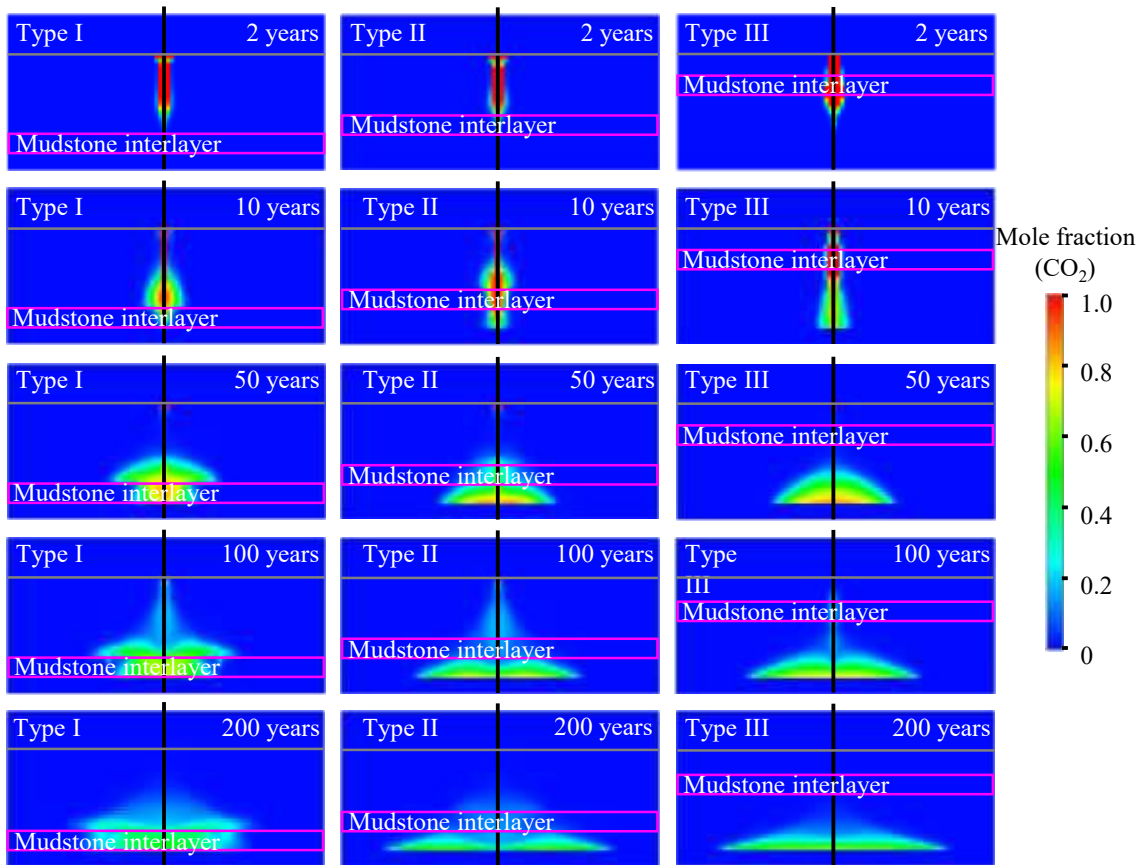


**Fig. 12.** Variation in CO<sub>2</sub> mole fraction distribution with time in three reservoir-caprock combinations.

ical barrier that restricts upward deformation and pressure-induced stress propagation toward the caprock. This configuration therefore exhibits a more confined mechanical response within the reservoir, contributing to an enhanced mechanical stability of the overlying caprock. Therefore, from the perspective of sequestration safety, the Type III configuration is the most favorable and should be prioritized in site selection.

The temporal evolution of CO<sub>2</sub> mole fraction during the sequestration process for the three types of reservoir-caprock combinations is illustrated in Fig. 12. Although injection depth is identical across all cases, differences in the relative positions of the reservoir and caprock lead to variations in migration pathways, diffusion behavior, and final CO<sub>2</sub> distribution. By the end of the 200-year simulation, residual CO<sub>2</sub> remains accumulated beneath the caprock in Type I and II, whereas in Type III, CO<sub>2</sub> is almost entirely retained below the mudstone interlayer, further indicating its superior sequestration security.

It should be noted that the present caprock evaluation primarily focuses on thickness and lateral continuity as first-order screening indicators of sealing capacity. Although breakthrough pressure is widely recognized as a critical parameter controlling caprock sealing performance, its quantitative determination is strongly influenced by mineral composition, pore size distribution, diagenetic processes, and temperature-pressure conditions. Under high-temperature and high-pressure environments, such effects may become even more pro-

nounced. Due to the lack of regionally consistent core-scale measurements and the uncertainties associated with estimating breakthrough pressure solely from well logging data, a direct calculation of breakthrough pressure is beyond the scope of this study. To better constrain breakthrough pressure variations and further validate caprock integrity under high-temperature and high-pressure conditions, future work should incorporate laboratory-based core experiments and detailed petrophysical analyses (Ye et al., 2025). In addition, further studies incorporating more detailed stratigraphic architectures, variable burial depths, and site-specific geological data will be valuable for further evaluating the impact of fine-scale heterogeneity on geomechanical behavior.

## 6. Conclusions

Saline aquifers are widely considered as promising candidates for CO<sub>2</sub> sequestration, yet comprehensive suitability evaluations at the basin scale remain limited in many offshore settings. Taking the Fushan Depression in the South China Sea as an example, this study presents an integrated assessment of saline aquifer sequestration potential based on geological, petrophysical and thermodynamic analyses within the IEAGHG evaluation framework. The main conclusions can be summarized as follows:

- 1) The saline aquifer system in the Fushan Depression generally satisfies the pressure-temperature conditions re-

quired to maintain CO<sub>2</sub> in a supercritical state, indicating that the basin as a whole is favorable for long-term and stable CO<sub>2</sub> sequestration.

- 2) Reservoir quality exhibits clear spatial and stratigraphic heterogeneity, whereas multiple stratigraphic intervals contain sand bodies with sufficient porosity, permeability and effective thickness. In the northeast (BJ, BL, HC, YA, and YU), suitable reservoirs are mainly found in the upper Ewz1 and Ewz2 intervals, while in the southwest (MT, CY and HG), favorable reservoirs are located in the lower Ewz3. These reservoirs collectively provide sequestration capacity and injectivity, demonstrating that high-quality sequestration reservoirs are widely developed at the basin scale.
- 3) Sealing capacity varies among stratigraphic intervals, with certain mudstone-dominated units exhibiting regionally effective caprock properties. For example, The Ewz2 interval shows the best sealing characteristics, particularly in BL and HC blocks. In contrast, other intervals show more limited sealing ability; for example, Ewz1 and Ewz3 generally lack sufficient caprocks, with only a few wells (like JF2, LIAN36, HC129, HG7, M17, YU3) meeting caprock requirements, highlighting the importance of caprock continuity and thickness as key controls on sequestration security.
- 4) By integrating the characteristics of reservoir and caprock, different reservoir-caprock combinations were identified and classified into three types across the study area. These combinations reflect systematic vertical assemblages rather than individual well-scale phenomena, providing a useful framework for classifying and comparing sequestration suitability in similar sedimentary basins.
- 5) Coupled geomechanical-fluid flow simulations indicate that reservoir pressurization and caprock response during CO<sub>2</sub> injection follow a staged temporal evolution. Type III combination, featuring upper mudstone interlayers, yields the lowest caprock stress and leakage risk. The upper interlayer acts as a secondary caprock, enhancing overall efficiency and sequestration security.

Overall, this study demonstrates that basin-scale integrated evaluation, combined with reservoir-caprock configuration analysis and numerical simulation, provides an effective approach for assessing the saline aquifer CO<sub>2</sub> sequestration potential and can be broadly applied to other sedimentary basins.

## Acknowledgements

This work was supported by the International Science & Technology Cooperation Program of Hainan Province (NO. GHYF2023004), the Science and Technology special fund of Hainan Province (No. ZDYF2024SHFZ147), the China Postdoctoral Science Foundation (No. 2022M710155), the National Natural Science Foundation of China (Nos. 42406233 and 42476238), and the Hainan Provincial Postdoctoral Research Funding Project.

## Conflicts of interest

The authors declare no competing interest.

**Open Access** This article is distributed under the terms and conditions of the Creative Commons Attribution (CC BY-NC-ND) license, which permits unrestricted use, distribution, and reproduction in any medium, provided the original work is properly cited.

## References

- Abbott, A. Plans resurrected to raise Venice above the encroaching sea. *Nature*, 2004, 427(6971): 184-184.
- Bachu, S. Screening and ranking of sedimentary basins for sequestration of CO<sub>2</sub> in geological media in response to climate change. *Environmental Geology*, 2003, 44(3): 277-289.
- Birkholzer, J. T., Zhou, Q. Basin-scale hydrogeologic impacts of CO<sub>2</sub> storage: Capacity and regulatory implications. *International Journal of Greenhouse Gas Control*, 2009, 3(6): 745-756.
- Castelletto, N., Ferronato, M., Gambolati, G., et al. Can Venice be raised by pumping water underground? A pilot project to help decide. *Water Resources Research*, 2008, 44(1): W01408.
- Chadwick, A., Arts, R., Bernstone, C., et al. Best practice for the storage of CO<sub>2</sub> in saline aquifers-observations and guidelines from the SACS and CO2STORE projects. Keyworth, Nottinghamshire, England, British Geological Survey, 2008.
- Chen, B., Mehana, M. Z., Pawar, R. J. Quantitatively evaluating greenhouse gas leakage from CO<sub>2</sub> enhanced oil recovery fields. *Advances in Geo-Energy Research*, 2023, 7(1): 20-27.
- Chen, Y., Wu, S., Zhou, X., et al. Sensitivity of various forms of CO<sub>2</sub> sequestration to different parameters in saline aquifers in the Fushan depression based on numerical simulation. *Energy*, 2025, 319: 135092.
- Gibson-Poole, C. M., Svendsen, L., Underschultz, J., et al. Site characterisation of a basin-scale CO<sub>2</sub> geological storage system: Gippsland Basin, southeast Australia. *Environmental Geology*, 2008, 54(8): 1583-1606.
- Gorecki, C. D., Sorensen, J. A., Bremer, J. M., et al. Development of storage coefficients for determining the effective CO<sub>2</sub> storage resource in deep saline formations. Paper SPE 126444 Presented at SPE International Conference on CO<sub>2</sub> Capture, Storage, and Utilization, San Diego, California, USA, 2-4 November, 2009.
- Hao, S., Zhang, Y., Li, X., et al. Numerical simulation study on surface deformation in the process of CO<sub>2</sub> geological storage. *National Engineering Geology Academic Annual Conference 2015*, 2015: 320-326.
- Holloway, S. An overview of the underground disposal of carbon dioxide. *Energy Conversion and Management*, 1997, 38: S193-S198.
- Huo, C. Evaluation of the potential for sub-seabed CO<sub>2</sub> storage in China's offshore areas and research on storage zones. Dalian, Dalian Maritime University, 2014. (in Chinese)
- Kumar, S., Foroozesh, J., Edlmann, K., et al. A comprehensive

- review of value-added CO<sub>2</sub> sequestration in subsurface saline aquifers. *Journal of Natural Gas Science and Engineering*, 2020, 81: 103437.
- Li, P., Zhou, D., Zhang, C., et al. Assessment of the effective CO<sub>2</sub> storage capacity in the Beibuwan Basin, offshore of southwestern PR China. *International Journal of Greenhouse Gas Control*, 2015, 37: 325-339.
- Liu, E., Wang, H., Li, Y., et al. Sedimentary characteristics and tectonic setting of sublacustrine fans in a half-graben rift depression, Beibuwan Basin, South China Sea. *Marine and Petroleum Geology*, 2014, 52: 9-21.
- Mathieson, A., Wright, I., Roberts, D., et al. Satellite imaging to monitor CO<sub>2</sub> movement at Krechba, Algeria. *Energy Procedia*, 2009, 1(1): 2201-2209.
- Nordbotten, J. M., Celia, M. A., Bachu, S., et al. Semianalytical solution for CO<sub>2</sub> leakage through an abandoned well. *Environmental Science & Technology*, 2005, 39(2): 602-611.
- Onuma, T., Ohkawa, S. Detection of surface deformation related with CO<sub>2</sub> injection by DInSAR at In Salah, Algeria. *Energy Procedia*, 2009, 1(1): 2177-2184.
- Qin, J., Zhong, Q., Tang, Y., et al. CO<sub>2</sub> storage potential assessment of offshore saline aquifers in China. *Fuel*, 2023, 341: 127681.
- Rahman, M. J., Fawad, M., Choi, J. C., et al. Effect of overburden spatial variability on field-scale geomechanical modeling of potential CO<sub>2</sub> storage site Smeaheia, offshore Norway. *Journal of Natural Gas Science and Engineering*, 2022, 99: 104453.
- Raza, A., Rezaee, R., Gholami, R., et al. A screening criterion for selection of suitable CO<sub>2</sub> storage sites. *Journal of Natural Gas Science and Engineering*, 2016, 28: 317-327.
- Rochelle, C. A., Camps, A. P., Long, D., et al. Can CO<sub>2</sub> hydrate assist in the underground storage of carbon dioxide? *Geological Society London Special Publications*, 2009, 319(1): 171-183.
- Rutqvist, J., Vasco, D. W., Myer, L. Coupled reservoir-geomechanical analysis of CO<sub>2</sub> injection and ground deformations at In Salah, Algeria. *International Journal of Greenhouse Gas Control*, 2010, 4(2): 225-230.
- Rutqvist, J., Wu, Y. S., Tsang, C. F., et al. A modeling approach for analysis of coupled multiphase fluid flow, heat transfer, and deformation in fractured porous rock. *International Journal of Rock Mechanics and Mining Sciences*, 2002, 39(4): 429-442.
- Rutqvist, J. The geomechanics of CO<sub>2</sub> storage in deep sedimentary formations. *Geotechnical and Geological Engineering*, 2012, 30(3): 525-551.
- Tomić, L., Karović-Maričić, V., Danilović, D., et al. Criteria for CO<sub>2</sub> storage in geological formations. *Podzemni Radovi*, 2018 (32): 61-74.
- Van der Meer, L. G. H. Investigations regarding the storage of carbon dioxide in aquifers in the Netherlands. *Energy Conversion and Management*, 1992, 33(5-8): 611-618.
- Vasco, D. W., Ferretti, A., Novali, F. Reservoir monitoring and characterization using satellite geodetic data: Interferometric synthetic aperture radar observations from the Krechba field, Algeria. *Geophysics*, 2008, 73(6): WA113-WA122.
- Wang, X., Li, M. J., Shi, Y., et al. Detailed oil-source correlation within the sequence and sedimentary framework in the Fushan Depression, Beibuwan Basin, South China Sea. *Petroleum Science*, 2025, 22(1): 90-109.
- Wang, X., Lu, Z., Li, M., et al. Petroleum charging history of the Paleogene sandstone reservoirs in the Huangtong Sag of the Fushan Depression, South China Sea. *Energies*, 2022, 15(4): 1374.
- Wei, B., Xie, R., Zhao, J., et al. Analysis of genesis of low resistivity reservoirs and method of fluid identification in Fushan Sag. *Journal of China University of Petroleum (Edition of Natural Science)*, 2024, 48(2): 57-66. (in Chinese)
- Ye, S., Song, X., Ma, Z., et al. A noise-resistant and annotation-free supervoxel-based algorithm for rapid segmentation of multiphase X-ray images. *Advances in Geo-Energy Research*, 2025, 16(1): 50-59.
- Zeng, B., Li, M. J., Wang, N., et al. Geochemistry and heterogeneous accumulation of organic matter in lacustrine basins: A case study of the Eocene Liushagang Formation in the Fushan Depression, South China Sea. *Petroleum Science*, 2022, 19(6): 2533-2548.
- Zeng, B., Lu, Z., Yang, T., et al. Hydrocarbon generation history of the Eocene source rocks in the Fushan Depression, South China Sea: Insights from a basin modeling Study. *Processes*, 2023, 11(7): 2051.
- Zhou, X., Wu, S., Bosin, A., et al. Evaluation of CO<sub>2</sub> hydrate storage potential in the Qiongdongnan Basin via combining the phase equilibrium mechanism and the volumetric method. *Advances in Geo-Energy Research*, 2024, 11(3): 220-229.